Vacuum 86 (2012) 1278–1283

Contents lists available at SciVerse ScienceDirect

Vacuum

journal homepage: www.elsevier.com/locate/vacuum

Engineering the tube size for an inner surface modification by plasma-based ion implantation

Y. Li [a,b], B.C. Zheng [a], M.K. Lei [a,*]

[a] Surface Engineering Laboratory, School of Materials Science and Engineering, Dalian University of Technology, Dalian 116024, China
[b] School of Science, Liaoning University of Technology, Jinzhou 121001, China

ARTICLE INFO

Article history:
Received 18 September 2011
Received in revised form
15 November 2011
Accepted 15 November 2011

Keywords:
Plasma-based ion implantation
Inner surface modification
Critical radius of tube (CRT)
Collisional fluid model
Optimum process parameters

ABSTRACT

In order to apply the inner surface modification of the tube component by plasma-based ion implantation (PBII) technique, the tube size has been characterized by introducing a characteristic parameter – the critical radius of tube (CRT) to optimize the process parameters of a grid-enhanced PBII technique for the nitrogen ion implantation onto the inner surface of an Fe–Cr–Ni stainless steel tube under the process conditions, including the plasma density of central plasma source, the steady pulse voltage, the grid electrode radius, and the processing pressure. The temporal sheath dynamics of the ion matrix sheath on the inner surface of the tube component modified by PBII were demonstrated by the collisional fluid model using the equations of ion continuity and ion motion, Poisson's equation, and Boltzmann's relationship of electron to determine the effective range of the process parameters. The optimum process parameters were found by the effect factors of the CRT which was bounded by the two important process parameters, i.e. the ion implantation dose and the processing time, for the engineering practice due to the available dependence on the surface modification effect in suitable costs.

1. Introduction

Plasma-based ion implantation (PBII) including plasma source ion implantation (PSII) [1,2] and plasma immersion ion implantation (PIII) [3,4] is a powerful technique for surface modification, because it eliminates the line-of-sight restrictions and removes the extremely shallow implanted depth limitation in comparison with conventional ion beam implantation. A lot of materials, such as metals, ceramics, semiconductors, as well as polymers, have been successfully modified, however, there are still many technical difficulties, such as modification uniformity and implanted ion dose enough due to the main problems of ion-matrix sheath overlap and implanted ion depletion [5,6], need to be solved when PBII is used to modify the components with complex shape, e.g. the tube with an inner surface.

Liu et al. [7,8] proposed a new method for inner surface modification by a grid-enhanced radio frequency (RF) PSII technique. In the central axis of a tube sample, an RF plasma was produced between a central cathode and a coaxial grid electrode. The RF plasma can diffuse through the grid electrode grounded out. When a negative pulsed voltage was biased on the tube sample, a uniform ion implantation on the inner surface of the tube sample can be realized using the ions accelerated within the diffused plasma region based on the PSII technique. Wang et al. [9,10] further made the corresponding theoretical studies for the grid-enhanced RF PSII technique with cylindrical geometry. A collisional fluid model was used to describe the ion sheath dynamics between the grid electrode and the inner surface of the tube sample. The effects of the ion-neutral collision within the diffused plasma on the implanted ion dose and impact energy were researched by solving the fluid equations for ions coupled with Boltzmann's assumption for electrons and Poisson's equation. It was found that the small gap distance between grid electrode and tube sample is favorable to increase the implanted ion dose and impact energy on the inner surface of the tube sample according to the qualitative relationship for the normalized PSII process parameters.

In order to promote engineering the grid-enhanced PBII technique, the theoretical study on the optimum PBII process bounded by the process parameters for the inner surface modification of the tube has been attempted on the basis of the temporal sheath dynamics of the ion-matrix sheath [10,11]. The two important process parameters, i.e. ion implantation dose and processing time, were accepted through the engineering practice due to an available dependence on the surface modification effect in suitable costs [12,13]. In this paper, a characteristic parameter – the critical radius of tube (CRT) was used to characterize the maximum size of the ion

* Corresponding author. Tel.: +86 41184707255; fax: +86 41184706192.
E-mail address: surfeng@dlut.edu.cn (M.K. Lei).

0042-207X/$ – see front matter © 2011 Elsevier Ltd. All rights reserved.
doi:10.1016/j.vacuum.2011.11.014

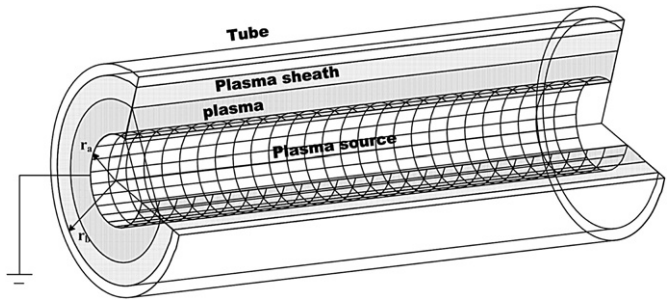

Fig. 1. The schematic diagram of the grid-enhanced plasma-based ion implantation apparatus for the inner surface modification of the tube component.

implanted tube under the process conditions, including the plasma density of central plasma source, the steady pulse voltage, the grid electrode radius, and the processing pressure, by the collisional fluid model using the equations of ion continuity and ion motion, Poisson's equation, and Boltzmann's relationship of electron for the grid-enhanced PBII technique.

2. Process conditions, model and simulation

The schematic diagram of the grid-enhanced PBII apparatus for the inner surface modification of the tube component is shown in Fig. 1. A central RF or microwave plasma source and a coaxial cylindrical grid electrode were arranged in a vacuum chamber, which was constructed by the tube component and the two end flanges. The RF plasma was established between the central cathode and the grounded grid electrode. Alternatively, the microwave plasma was produced by a central antenna through the grounded grid electrode. The plasmas were assumed to be homogeneous in the plasma sources. Therefore, the grid electrode radius r_a was the plasma source radius. The r_a and the radium of tube component r_b were designed by 2–20 cm and 3–50 cm, respectively. The typical plasma density n_0 and electron temperature T_e in the RF and microwave plasma sources were in the range from 1.0×10^9 ions/cm^3 to 5.0×10^9 ions/cm^3, and from 1 eV to 5 eV, respectively. The plasma between the grid electrode and the inner surface of the tube which diffused outward from the central plasma source was non-homogeneous. A trapezoidal-shape pulsed voltage with a steady value ϕ_p of -10 to -100 kV and a raising and falling time of 1.0 μs respectively was biased to the tube component. The voltage pulse width was 10 μs and the repetition frequency f was 2×10^2 Hz. The processing pressure P with pure nitrogen gas addition was maintained at 1×10^{-2} Pa, and only one type of ions N_2^+ was formed in the plasma. At the process time τ beginning, the pulsed voltage was applied on the tube component, then the ion sheath of the diffused plasma expanded inward until it reached the grounded grid electrode. When the sheath from the plasma source stopped expanding, the nitrogen ions will be extracted from the plasma source through the grid electrode and accelerated directly onto the inner surface of the tube component.

The ion sheath dynamics within the diffused plasma region between the grid electrode and the inner surface of the tube component were studied by the collisional fluid model. The plasma between the grid and the inner surface of tube was calculated from the variable mobility model of low-pressure diffusion solutions. The Child–Langmuir law with a space-charge-limited current was derived from the ion energy equation, flux conservation equation, and Poisson's equation. Like the Child–Langmuir law, the space charge effect was considered in the collisional fluid model by using the equations of ion continuity and ion motion, Poisson's equation, and Boltzmann's relationship of electron for the grid-enhanced PSII technique. The effect of the secondary electrons on the space charge was ignored due to the very low electron density resulted by the high pulsed voltage in the sheath. The grounded grid electrode restricted the sheath away to the central plasma source, and no hollow cathode plasma was produced. The collisional fluid model of the ion sheath dynamics is given by [10]

$$\begin{aligned}
&\frac{\partial n_i}{\partial t}+\frac{1}{r}\frac{\partial}{\partial r}(rn_iv_i)=0,\\
&\frac{\partial v_i}{\partial t}+v_i\frac{\partial v_i}{\partial r}=-\frac{e}{M_i}\frac{\partial\phi}{\partial r}-\frac{F_c}{M_i},\\
&\frac{1}{r}\frac{\partial}{\partial r}r\frac{\partial\phi}{\partial r}=-\frac{e}{\varepsilon_0}(n_i-n_e),\\
&n_e=n_0\exp\left(\frac{e\phi}{kT_e}\right),
\end{aligned}\tag{1}$$

where, n_i is ion density, n_e is electron density, n_0 is plasma density of the plasma source, T_e is electron temperature, t is implantation time during a voltage pulse, v_i is ion velocity, M_i is mass of a nitrogen ion N_2^+, ϕ is potential within the sheath, e is electron charge, ε_0 is permittivity of free space, k is Boltzmann constant. F_c is collision drag force, which was written [14] as

$$F_c=\frac{\pi}{2}M_i\gamma v_i \tag{2}$$

where, $\gamma=|v_i|/\lambda_i$ is ion-neutral collision rate, $\lambda_i=1/(n_g\sigma_m)$ is mean free path, n_g is neutral gas density, which is determined by its pressure P, σ_m is ion-neutral momentum transfer cross-section, for which the following formula adjusted to fit the date [15] from

$$\begin{cases}
\sigma_m=\left(56.46+\dfrac{38.34}{\sqrt{\varepsilon}}\right)\times10^{-16}\ \text{cm}^2 & (\varepsilon\geq10^{-4}\ \text{eV}),\\
\sigma_m=3.89\times10^{-13}\ \text{cm}^2 & (\varepsilon<10^{-4}\ \text{eV}),
\end{cases}\tag{3}$$

where, ε is laboratory energy of N_2^+ expressed in eV. And a constant cross-section was used when the ions energy is less than 10^{-4} eV.

The implanted ion current J is determined by the instantaneous n_i and v_i of the implanted ion, which is given by

$$J=en_iv_i. \tag{4}$$

In the grid-enhanced PBII process, we assume that all the impact ions onto the inner surface of the tube component can be implanted during the pulse-on time of the pulsed voltage, e.g. $t=10$ μs, and the pulse-off time is so long that the diffused plasma between the grid electrode and the inner surface of the tube can recover to its initial state before beginning of the next pulse. The sputtering effect can be ignored under the process conditions, i.e. high-pulsed voltage and lower pressure. Therefore, the relationship between the two important process parameters, as ion implantation dose D_T and processing time τ, is obtained

$$D_T=f\tau D_0=f\tau\int_0^t J\,dt, \tag{5}$$

where, D_0 is the ion implantation dose during one voltage pulse.

The boundary conditions of the process model are

$$\begin{aligned}
&n_i|_{r=r_a}=n_0,\\
&v_i|_{r=r_a}=0,\\
&\phi|_{r=r_a}=0,\\
&\phi|_{r=r_b}=\phi_t.
\end{aligned}\tag{6}$$

We adopt the variable mobility model of low-pressure diffusion solutions [16] to obtain the initial ion density and velocity

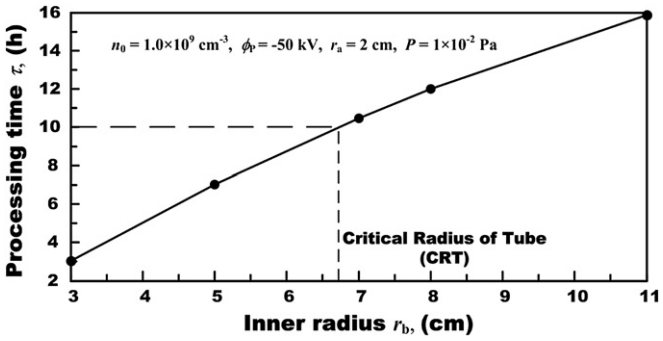

Fig. 2. The maximum size of the inner radius of the tube component ion implanted over a threshold of ion implantation dose D_T of 1×10^{17} ions/cm^2 during a processing time τ up to 16 h under the process conditions: $n_0 = 1\times10^9$ ions/cm^3, $T_e = 2$ eV, $\phi_p = -50$ kV, $r_a = 2$ cm, and $P = 1\times10^{-2}$ Pa.

distribution, but the ion-neutral momentum transfer cross-section is used by the experimental fitting data from Eq. (3) [15].

For an Fe–Cr–Ni stainless steel modified by nitrogen ion implantation, ion implantation dose D_T should achieve a level enough of 10^{17} ions/cm^2 in order to get a significant modification effect [12,13]. In the grid-enhanced PBII process, the ion implantation dose must be large enough during the reasonable processing time τ. An ion implantation dose of 1×10^{17} ions/cm^2 was achieved in the whole process, and the whole processing time τ could not be too long, which was set no more than 10 h.

Using the above initial and boundary conditions, Eq. (1) was solved with a finite difference method to obtain the data of implanted ion density, ion impact velocity, implanted ion current, temporal evolution of the sheath, and ion implantation dose. The space step and time step are $\Delta r = 5\times10^{-2}$ cm, $\Delta t = 2.5\times10^{-4}$ μs in the process simulation, respectively.

3. Results and discussion

3.1. Critical radius of tube (CRT)

In order to characterize the extreme size of the tube component ion implanted under the process conditions, such as the plasma density n_0 and electron temperature T_e of central plasma source, the steady pulse voltage ϕ_p, the grid electrode radius r_a, and the processing pressure P, the critical radius of tube (CRT) was obtained from the relationship between the ion implantation dose D_T and the processing time τ. Fig. 2 shows the maximum size of the inner radius r_b of the tube ion implanted over a threshold of ion implantation dose of 1×10^{17} ions/cm^2 during a processing time τ up to 16 h under the process conditions: $r_a = 2$ cm, $n_0 = 1.0\times10^9$ ions/cm^3, $T_e = 2$ eV, $\phi_p = -50$ kV, and $P = 1\times10^{-2}$ Pa. With increasing the tube radius r_b, the processing time τ is prolonged in a parabolical orbit. For a tube of the $r_b = 6.7$ cm, an enough ion implantation dose of $D_T = 1\times10^{17}$ ions/cm^2 needs a processing time of $\tau = 10$ h, namely, more than the 6.7-cm radius tube can not obtain effective modification effect within 10 h. Therefore, the tube modified by ion implantation possesses a maximal size under the certain process conditions mentioned above. The maximum size of the inner radius of the tube, called as CRT, is 6.7 cm. Moreover, the minimum size of the tube is not limited in principle, which is only more than the radius of the plasma source naturally.

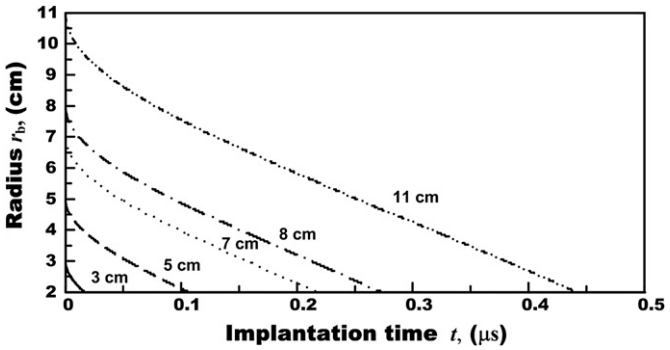

Fig. 4. The sheath boundary shifting during the implantation time t in the different tube component with a radius from 3 cm to 11 cm.

For the threshold of $D_T = 1\times10^{17}$ ions/cm^2 during a maximal processing time of $\tau = 10$ h, the implanted ion current J dependent on the instantaneous implanted ion density n_i and the ion impact velocity v_i was analyzed for the tube component ion implanted with the different tube radius r_b under $r_a = 2$ cm, $n_0 = 1.0\times10^9$ ions/cm^3, $T_e = 2$ eV, $\phi_p = -50$ kV, and $P = 1\times10^{-2}$ Pa. Fig. 3 shows the temporal evolution of the instantaneous implanted ion density n_i in the different tube with a radius from 3 cm to 11 cm. The n_i value decreased sharply from a high density and then stabilized to a low constant for all the tubes, moreover, the steady n_i value in the smaller radius tube was bigger. For the tube of the $r_a = 3$ cm, the n_i value was observed as 8.8×10^7 ions/cm^3, but the $n_i = 1.3\times10^7$ ions/cm^3 only for that of the $r_a = 11$ cm. The sheath expanded during the voltage pulse width rapidly to the grid electrode after the pulsed voltage was biased. The sheath boundary shifting during the implantation time t in the different tube with a radius from 3 cm to 11 cm is shown in Fig. 4. The sheath

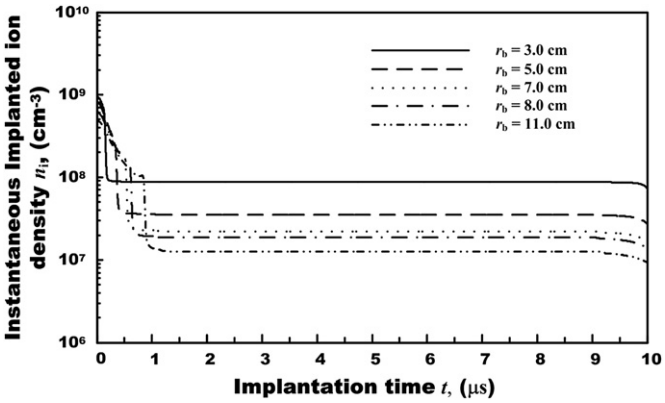

Fig. 3. The temporal evolution of the instantaneous implanted ion density n_i in the different tube component with a radius from 3 cm to 11 cm.

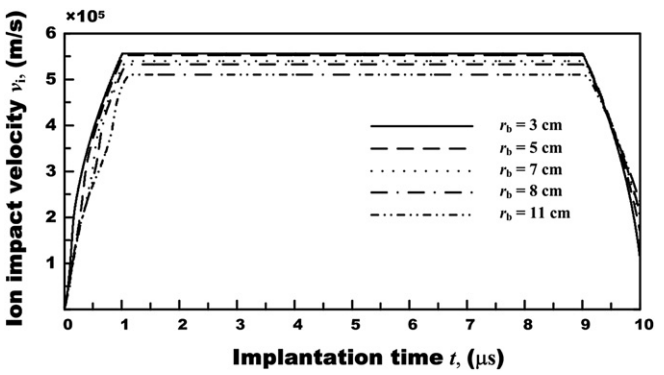

Fig. 5. The ions impact velocity v_i during the implantation time t in the different tube component with a radius from 3 cm to 11 cm.

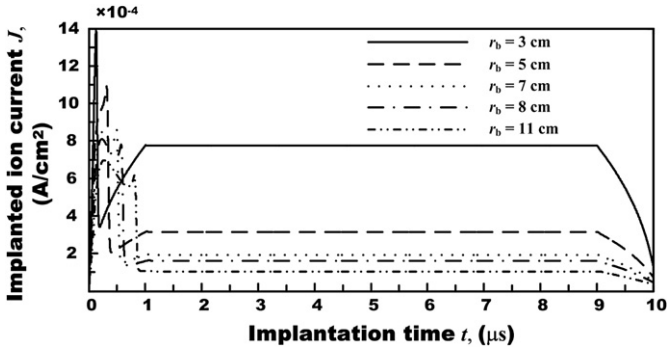

Fig. 6. The temporal evolution of the implanted ion current J in the different tube component with a radius from 3 cm to 11 cm.

boundaries with the t moved by a similar expanding velocity of 10^5 m/s in the different radius tubes. For the larger tube of the $r_a = 11$ cm, the sheath boundary reached the central plasma source within a shorter time of 0.45 μs than that of the voltage pulse width of 10 μs. The additional ions were extracted from the central plasma source into the sheath between the grid electrode and the inner surface of the tube by the electric field force in a longer range of the voltage pulse. Because the distance between the plasma source and the inner surface of the tube is shorter for the small tube, the implanted ions will experience the slight divergence along the radial direction and the few collision when they traverse from the grid electrode to the inner surface of the tube, leading to the high steady value of the instantaneous implanted ion density in the small tube [17,18]. The ions impact velocity v_i during the implantation time t in the different tube with a radius from 3 cm to 11 cm is shown in Fig. 5. The change of the v_i was corresponding to that of the trapezoidal-shape pulsed voltage with the raising, steady and falling times. With increasing the r_b, the v_i decreased. According to Eq. (4), the temporal evolution of the implanted ion current J in the different tube with a radius from 3 cm to 11 cm is showed in Fig. 6. For the tube of the $r_a = 3$ cm, the peak and steady values of the implanted ion current J were observed as 13.99×10^{-4} A/cm^2 and 7.76×10^{-4} A/cm^2, but only 6.97×10^{-4} A/cm^2 and 1.04×10^{-4} A/cm^2 for the tube of the $r_a = 11.0$ cm. The steady ion current occupied most of the whole voltage pulse, leading to the higher ion implantation dose in the smaller tube obtained by Eq. (5).

When the size of the central RF or microwave plasma source in the grid-enhanced PBII technique is certain, the J is smaller in the larger tube due to the longer distance between the plasma source and the inner surface of the tube component. It is well established that in the sheaths of the plasma, the average ion velocity decreased rapidly as the distance from an electrode increased [19]. The tube size for the inner surface modification by PBII is large enough that can not be modified over the threshold of ion implantation dose of 1×10^{17} ions/cm^2 required within a maximal processing time τ of 10 h. The CRT is introduced as a characteristic parameter to characterize the maximum size of the ion implanted tube under the plasma density of central plasma source, the steady pulse voltage, the grid electrode radius, and the processing pressure.

3.2. Effect factors of critical radius of tube

In order to estimate systematically the effect factors of the CRT, the typical process conditions: $n_0 = 1.0 \times 10^9$ ions/cm^3, $T_e = 2$ eV, $\phi_p = -50$ kV, $r_a = 2$ cm, and $P = 1 \times 10^{-2}$ Pa were sampled as a base of the conditions to compare with the separately changed process parameters in the process. The changed process conditions were as

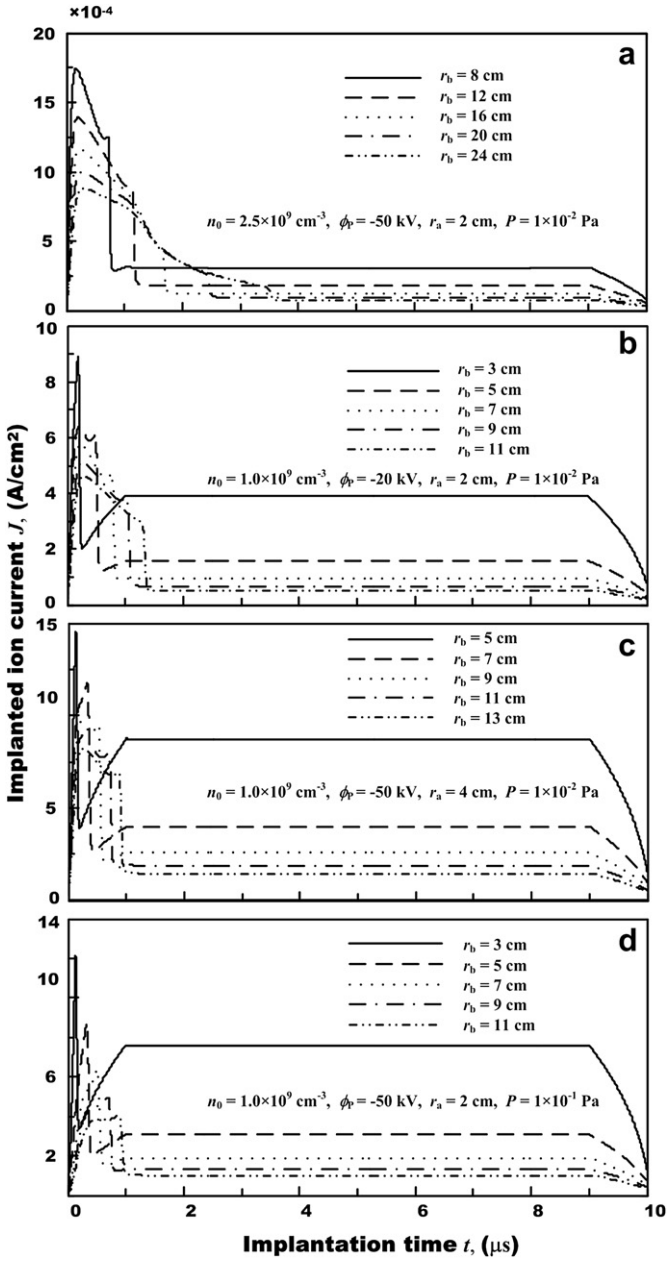

Fig. 7. The temporal evolution of the implanted ion current J in the different tube with a radius from 3 cm to 24 cm under the changed process conditions: $n_0 = (1–2.5) \times 10^9$ ions/cm^3, $T_e = 2$ eV, $\phi_p = -50$ to -20 kV, $r_a = 2–4$ cm, and $P = 1 \times 10^{-2}–1 \times 10^{-1}$ Pa.

following: $n_0 = (1.0–2.5) \times 10^9$ ions/cm^3, $\phi_p = -50$ to -20 kV, $r_a = 2–4$ cm, and $P = 1 \times 10^{-2}–1 \times 10^{-1}$ Pa. Fig. 7 shows the temporal evolution of the implanted ion current J in the different tube under the changed process conditions, compared with that under the typical process conditions as shown in Fig. 6. When the n_0 individually increased from 1.0×10^9 ions/cm^3 to 2.5×10^9 ions/cm^3, the peak and steady values of the J increased from 8.10×10^{-4} A/cm^2 and 1.60×10^{-4} A/cm^2 to 17.43×10^{-4} A/cm^2 and 3.09×10^{-4} A/cm^2, for the tube of the $r_b = 8.0$ cm [Fig. 7(a)]. When the ϕ_p individually decreased from -50 kV to -20 kV, the peak and steady J decreased from 8.61×10^{-4} A/cm^2 and 1.92×10^{-4} A/cm^2 to 5.76×10^{-4} A/cm^2 and 0.94×10^{-4} A/cm^2, for the tube of the $r_b = 7.0$ cm [Fig. 7(b)]. With individually increasing the r_a from 2 cm to 4 cm, the peak and steady J increased from 8.61×10^{-4} A/cm^2

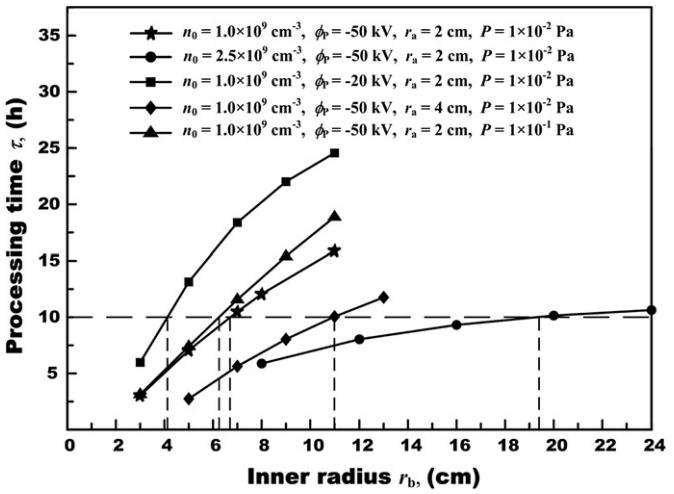

Fig. 8. The critical radius of the tube (CRT) in the grid-enhanced PBII process over the threshold of ion implantation dose D_T of 1×10^{17} ions/cm^2 under all the changed effect factors: $n_0 = (1–2.5)\times10^9$ ions/cm^3, $T_e = 2$ eV, $\phi_p = -50$ to -20 kV, $r_a = 2–4$ cm, and $P = 1\times10^{-2}–1\times10^{-1}$ Pa.

and 1.92×10^{-4} A/cm^2 to 11.79×10^{-4} A/cm^2 and 3.97×10^{-4} A/cm^2, for the tube of the $r_b = 7.0$ cm [Fig. 7(c)]. With individually increasing the P from 1×10^{-2} Pa to 1×10^{-1} Pa, the peak and steady J decreased from 11.09×10^{-4} A/cm^2 and 3.10×10^{-4} A/cm^2 to 8.80×10^{-4} A/cm^2 and 3.09×10^{-4} A/cm^2, for the tube of the $r_b = 5.0$ cm [Fig. 7(d)]. The higher n_0 can effectively increase the instantaneous n_i, leading to the higher J. The lower ϕ_p can weaken the electric field in the sheath, thereby decrease the v_i, reducing the J. A large size of the central plasma source can provide a shorter distance between the plasma source and the inner surface of the tube, however, the large-area plasma source is one of the interesting questions for plasma science and engineering due to principle and technological limitations. The linear RF and microwave plasma sources were developed and applied with a limitedly small size [20–22]. The higher P can lower the v_i which was caused by the more severe collisions, leading to the lower J.

According to the CRT relative to the D_T and the τ, the CRT in the grid-enhanced PBII process over the threshold of $D_T = 1\times10^{17}$ ions/cm^2 under all the changed effect factors is summarized in Fig. 8. The n_0 of the central plasma source has a significant effect on the CRT in the process, otherwise, the P has a slight effect on the CRT. When the n_0 individually increased from 1.0×10^9 ions/cm^3 to 2.5×10^9 ions/cm^3, the CRT increased from 6.7 cm to 19.4 cm, for the tube of the $r_a = 2$ cm. Further increasing the n_0 to 3.0×10^9 ions/cm^3, the CRT was obtained as 50 cm, which was about one order more than that with $n_0 = 1.0\times10^9$ ions/cm^3. When the ϕ_p individually decreased from -50 kV to -20 kV, the CRT decreased from 6.7 cm to 4.1 cm, for the tube of the $r_a = 2$ cm. Although an increase of the ϕ_p can increase the CRT, the change was limited. The ϕ_p in the process was less than -100 kV in the conventional ion beam implantation, however, the CRT is only increased to 10.4 cm for the tube of the $\phi_p = -100$ kV [23,24]. When the r_a individually increased from 2 cm to 4 cm, the CRT increased from 6.7 cm to 11.0 cm. With individually increasing the P from 1×10^{-2} Pa to 1×10^{-1} Pa, the CRT was not significantly changed as 6.7 cm and 6.3 cm. The optimum process parameters of the grid-enhanced PBII technique for the inner surface modification of the tube are listed in Table 1. For the inner surface modification by the grid-enhanced PBII process, the tube size was determined from the radius of the plasma source, as the radius of the grid electrode r_a, to the CRT which mainly depends on the n_0 of central plasma source and the ϕ_p. In the process under the changed process conditions, the maximum size of the ion implanted tube component was less than 50 cm in radius.

Table 1
The optimum process parameters of the grid-enhanced plasma-based ion implantation technique for the inner surface modification of the tube component.

n_0 (ions/cm^3)	ϕ_p (−kV)	r_a (cm)	P (Pa)	Critical radius of tube (cm)
$(1–3)\times10^9$	50	2	1×10^{-2}	$6.7 < CRT \leq 50.0$
1×10^9	20–100	2	1×10^{-2}	$4.1 < CRT \leq 10.4$
1×10^9	50	2–20	1×10^{-2}	$6.7 < CRT \leq 50.0$
1×10^9	50	2	$1\times10^{-2}–1\times10^{-1}$	$6.3 < CRT \leq 6.7$

The optimum process parameters of the grid-enhanced PBII technique for the inner surface modification of the tube were found based on characterization of the tube size by the CRT, which is derived from the temporal sheath dynamics of the ion-matrix sheath, according to the collisional fluid model using the equations of ion continuity and ion motion, Poisson's equation, and Boltzmann's relationship of electron. The determination of the main effect factors was attributed to demonstrating the effective range in the n_0 of central plasma source, the ϕ_p, the r_a, and the P, instead of the qualitative relationship for the normalized parameters [10,11]. The two important process parameters, i.e. ion implantation dose D_T and processing time τ, through the engineering practices were reasonably considered to optimize the process parameters due to available dependence on the surface modification effect in suitable costs.

4. Conclusions

(1) The critical radius of tube (CRT) was induced as a characteristic parameter to characterize the maximum size of the ion implanted tube component by the grid-enhanced PBII technique under the plasma density of central plasma source, the steady pulse voltage, the grid electrode radius, and the processing pressure.
(2) The plasma density of central plasma source and the steady pulse voltage were determined as the two main effect factors, according to the temporal sheath dynamics of the ion-matrix sheath by the collisional fluid model using the equations of ion continuity and ion motion, Poisson's equation, and Boltzmann's relationship of electron.
(3) The optimum process parameters of the grid-enhanced PBII technique for the inner surface modification of the tube component were found based on characterization of the tube size by the critical radius of tube (CRT), bounded by the two important process parameters, as ion implantation dose and processing time, through the engineering practices.

Acknowledgements

We acknowledge contributory discussions of Dr. Z.L. Dai, and Mr. Z.Y. Wang, and Mr. Z.P. Zhang in this research. This work is supported by the National Science Foundation of China under Grant No. 50725519.

References

[1] Conrad JR. Mater Sci Eng A 1989;116:197–203.
[2] Kondyurin A, Karmanov V, Guenzel R. Vacuum 2001;64:105–11.
[3] Collins GA, Hutchings R, Tendys J. Mater Sci Eng A 1991;139:171–8.
[4] Lei MK, Chen JD, Wang Y, Zhang ZL. Vacuum 2000;57:327–38.
[5] Sheridan TE. J Appl Phys 1993;74:4903–6.
[6] Sun M, Yang SZ, Li B. J Vac Sci Technol A 1996;14:367–9.
[7] Liu B, Liu CZ, Cheng DJ, Zhang GL, He R, Yang SZ. Nucl Instr Meth B 2001;184:644–8.

[8] Liu B, Zhang GL, Cheng DJ, Liu CZ, He R, Yang SZ. J Vac Sci Technol A 2001;19:2958–62.
[9] Wang JL, Zhang GL, Fan SH, Yang WB, Yang SZ. Chin Phys Lett 2002;19:1473–5.
[10] Wang JL, Zhang GL, Fan SH, Yang WB, Yang SZ. J Phys D 2003;36:1192–7.
[11] Zeng XC, Kwok TK, Liu AG, Chu PK, Tang BY. J Appl Phys 1998;83:44–9.
[12] Lei MK, Yuan LJ, Liu FL, Zhang ZL, Dai LS. Mater Mech Eng (Jixie Gongcheng Cailiao) 1995;19:29–30. 49.
[13] Lei MK, Zhu XP, Wang XJ. Oxid Metals 2002;58:361–74.
[14] Sheridan TE, Goeckner MJ. J Appl Phys 1995;77:4967–72.
[15] Phelps AV. J Phys Chem Ref Data 1991;20:557–73.
[16] Lieberman MA, Lichtenberg AJ. New Jersey, John Wiley & Sons Inc.; 2005. p. 144–6.
[17] Fu RKY, Fu KL, Tian XB, Chu PK. J Vac Sci Technol A 2004;22:356–60.
[18] Hubbard P, Dowey SJ, Partridge JG, Doyle ED, McCulloch DG. Surf Coat Technol 2010;204:1151–7.
[19] Goeckner MJ, Goree J, Sheridan TE. Phys Fluids B 1992;4:1663–70.
[20] Baránkova H, Bárdoš L, Berg S. Vacuum 1995;46:1433–8.
[21] Yoshiki H. Vacuum 2010;84:559–63.
[22] Rahman M, Glukhoy Y, Popov G, Usenko A, Walitzki HJ. Surf Coat Technol 2005;196:172–9.
[23] Kikkawa S, Sugiyama H, Ohmura T, Kanamaru F, Hinomura T, Nasu S. Vacuum 1996;47:863–6.
[24] Tagliente MA, Falcone R, Mello D, Esposito C, Tapfer L. Nucl Instr Meth B 2001;179:42–54.